Annals of Hepatology 30 (2025) 101743

Contents lists available at ScienceDirect

Annals of Hepatology

journal homepage: www.elsevier.es/annalsofhepatology

Original article

Assessing liver fibrosis in chronic liver disease: Comparison of diffusion-weighted MR elastography and two-dimensional shear-wave elastography using histopathologic assessment as the reference standard

Li Yang[a,b,1], Guofeng Zhou[a,1], Liheng Liu[a], Shengxiang Rao[a], Wentao Wang[a], Kaipu Jin[a], Caixia Fu[c], Mengsu Zeng[a], Ying Ding[a,*]

[a] Department of Radiology, Shanghai Institute of Medical Imaging, Zhongshan Hospital, Fudan University, Shanghai, PR China
[b] Department of Radiology, Xiamen Branch, Zhongshan Hospital, Fudan University, Xiamen, PR China
[c] MR Application Development, Siemens Shenzhen Magnetic Resonance Ltd, Shenzhen, PR China

ARTICLE INFO

Article History:
Received 9 May 2024
Accepted 23 August 2024
Available online 9 December 2024

Keywords:
Liver fibrosis
Elastography
Diffusion-weighted imaging MRI-based virtual elastography
Virtual shear modulus
2D shear-wave elastography
Liver stiffness measurement

ABSTRACT

Introduction and Objectives: Liver stiffness measurement (LSM) by two-dimensional shear-wave elastography (2D SWE) is a well-established method for assessing hepatic fibrosis. Diffusion-weighted imaging (DWI) can be converted into virtual shear modulus (μ_{Diff}) to estimate liver elasticity. The purpose of this study was to correlate and compare the diagnostic performance of DWI-based virtual elastography and 2D SWE for staging hepatic fibrosis in patients with chronic liver disease, using histopathologic assessment as the reference standard.

Patients and Methods: This retrospective study included 111 patients who underwent preoperative multiple b-value DWI and 2D SWE. The μ_{Diff} was calculated using DWI acquisition with b-values of 200 and 1,500 /mm^2, and LSM was obtained by 2D SWE. Correlation between μ_{Diff} and LSM was assessed, as well as the correlation between these noninvasive methods and histologic fibrosis stages. The diagnostic efficacy of μ_{Diff} and LSM for staging liver fibrosis was compared with receiver operating characteristic (ROC) curve analysis.

Results: There was a significant positive correlation between μ_{Diff} and LSM (rho= 0.48, $P < 0.001$). μ_{Diff} (rho= 0.54, $P < 0.001$) and LSM (rho= 0.76, $P < 0.001$) were positively correlated with liver fibrosis stages. Areas under the curves (AUCs) of μ_{Diff} and LSM, respectively, were 0.81 and 0.90 for significant fibrosis, 0.89 and 0.98 for advanced fibrosis, and 0.77 and 0.91 for cirrhosis. The AUCs of 2D SWE for diagnosing advanced fibrosis and cirrhosis were significantly higher than those of μ_{Diff} ($P < 0.05$ for both).

Conclusions: LSM by 2D SWE yields larger AUCs compared to μ_{Diff} obtained from DWI-based virtual elastography for various stages of liver fibrosis. LSM is superior to μ_{Diff} in predicting advanced fibrosis and cirrhosis.

© 2024 Fundación Clínica Médica Sur, A.C. Published by Elsevier España, S.L.U. This is an open access article under the CC BY-NC-ND license (http://creativecommons.org/licenses/by-nc-nd/4.0/)

1. Introduction

Liver fibrosis is associated with increased morbidity and mortality from chronic liver disease (CLD) worldwide [1]. As the disease progresses over time, liver fibrosis may develop to hepatocellular carcinoma and hepatic insufficiency [1,2]. Early detection and accurate staging of liver fibrosis provide a window for early interventions to halt or even reverse disease progression [2–4]. Therefore, a reliable diagnosis of hepatic fibrosis is pivotal for the management, surveillance, and prognosis of patients with CLD.

Although histologic assessment is considered the gold standard for diagnosing hepatic fibrosis, liver biopsy is invasive and limited by sample variability, interobserver reproducibility, and some complications, such as hemorrhage and pain [5,6]. In this context, various non-invasive tools, such as serum fibrosis biomarkers ultrasound-based or magnetic resonance imaging-based techniques, are used to stage liver fibrosis [2,7–9].

Liver stiffness measurement (LSM) using transient elastography, two-dimensional shear wave elastography (2D SWE), or MR elastography (MRE) is a well-established method for stratifying liver fibrosis in patients with CLD [2,8,10]. This technique measures liver stiffness

Abbreviations: ADC, apparent diffusion coefficient; AUC, areas under the curve; CI, confidence interval; CLD, chronic liver disease; DWI, diffusion-weighted imaging; ICC, intraclass correlation coefficient; IQR, interquartile range; LSM, liver stiffness measurement; MRI, magnetic resonance imaging; MRE, magnetic resonance elastography; ROC, receiver operating characteristic; ROI, region of interest; sADC, shifted apparent diffusion coefficient; 2D SWE, two-dimensional shear-wave elastography; uDiff, DWI-based virtual shear modulus; μMRE, shear modulus of magnetic resonance elastography

* Corresponding author.
E-mail address: ding.ying@zs-hospital.sh.cn (Y. Ding).

[1] Li Yang and Guofeng Zhou contributed equally to this work.

https://doi.org/10.1016/j.aohep.2024.101743
1665-2681/© 2024 Fundación Clínica Médica Sur, A.C. Published by Elsevier España, S.L.U. This is an open access article under the CC BY-NC-ND license (http://creativecommons.org/licenses/by-nc-nd/4.0/)

by quantifying the speed of wave propagation within the liver [8]. The propagation velocity is positively correlated with liver stiffness, which increases with the progression of fibrosis stages [8,11,12]. Moreover, 2D SWE and MRE have been recommended as accurate and reliable methods for staging liver fibrosis [2,10–12].

Diffusion-weighted imaging (DWI) enables a noninvasive assessment of microscopic diffusive water movements by measuring apparent diffusion coefficient (ADC) [13]. It has been reported that ADC values significantly decreased as liver fibrosis increased [14–16]. Moreover, recent studies revealed water diffusivity was strongly correlated with tissue elasticity in the liver [17,18]. Specifically, shifted ADC (sADC) was calculated from DWI acquired with optimized b values of 200 and 1500 s/mm^2 that reflected Gaussian and non-Gaussian diffusion and then converted to DWI-based virtual shear modulus (μ_{Diff}) [17]. Shear modulus of MRE (μ_{MRE}) was found to have a significant correlation with sADC and μ_{Diff} [17,18]. Thus DWI-based virtual MRE was proposed as a surrogate for MRE in liver fibrosis staging [17,18]. Importantly, DWI can be easily implemented in clinical abdominal MRI without requiring additional mechanical drivers like MRE.

To the best of our knowledge, no studies have been published on the comparison of DWI-based virtual MRE and 2D SWE for diagnosing liver fibrosis. Therefore, the purpose of our study was to correlate and compare the diagnostic accuracy of DWI-based virtual MRE and 2D SWE for liver fibrosis staging in patients with CLD, using histological assessment as the reference standard.

2. Material and Methods

2.1. Patients

Between July 2015 and July 2018, 171 consecutive patients (age range, 24–84 years) with focal liver tumors who underwent preoperative 2D-SWE and abdominal MRI, including multi-b-value DWI, were reviewed. The inclusion criteria were i) availability of DWI sequence with b values of 200 and 1500 s/mm^2; ii) successful acquisition of 2D SWE; iii) with histologic liver fibrosis grading. Sixty patients were excluded for the following reasons: i) absence of histologic fibrosis staging (n = 19), ii) prior intervention therapy (n = 13), iii) unsatisfactory image quality of DWI owing to ghosting and distortion or substantial iron overload (n = 14), iv) liver tumors that larger than 5 cm occupying the right lobe might affect 2D SWE and DWI measurements (n = 12), v) with bile duct tumor thrombus (n = 2). Thus, the final study group enrolled 111 patients (80 men and 31 women; mean age, 55.6 ± 10.9 years; age range, 27–84 years).

2.2. MR imaging and analysis

MR imaging was performed on a 1.5T MR scanner (MAGNETOM Aera, Siemens, Erlangen, Germany) with a phased array body coil. Multiple b-values DWI was obtained by using a free-breathing single-shot echo-planar sequence. Imaging parameters were as follows: repetition time/echo time, 8000 ms/63 ms; field of view, 380 × 308 mm^2; matrix,128 × 128; section thickness, 5 mm, and acquisition time, 2 min 4 s. The b values were 0, 200, 500, 1000, 1500, and 2000 s/mm^2 with number of signal averages of 1, 1, 2, 2, 3, 4, respectively, and diffusion encoded along the x, y, and z directions, but only b values of 200 and 1500 s/mm^2 were applied for this study.

An in-house developed program based on MATLAB (Mathworks, Natick, Mass) was applied to generate sADC and μ_{Diff} from the above-mentioned images with b values of 200 and 1500 s/mm^2, by using the following equations proposed in the literature [17,18]:

$$\text{sADC}\ (\text{mm}^2/\text{s}) = \text{In}(S_{200}/S_{1500})/1300,$$

$$\mu_{Diff}(\text{kPa}) = \alpha \text{sADC}(\text{mm}^2/\text{sec}) + \beta,$$

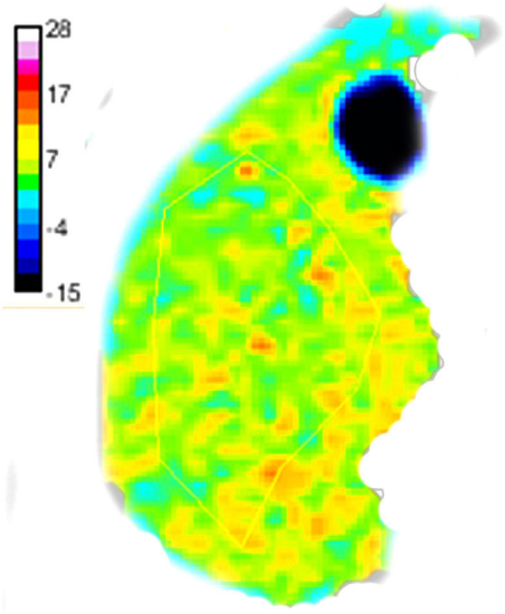

Fig. 1. Examples of placement of region of interest in the liver parenchyma on DWI-based virtual shear modulus (μ_{Diff}).

where S_{200} and S_{1500} are the image signals with b values of 200 and 1500 s/mm^2, respectively, sADC is the shifted ADC, and α and β are calibration coefficients [17,18].

Two abdominal radiologists independently analyzed the reconstructed virtual MRE maps using ITK-SNAP software (http://www.itksnap.org) blinded to the clinical and histopathological findings. μ_{Diff} were manually measured with freehand regions of interest (ROIs) on the right liver lobe in four continuous slices, avoiding the large vessels, focal lesions, liver margin, and image artifacts or distortions [8] (Fig. 1), and the averaged value were calculated for final analysis.

2.3. 2D SWE

Patients were fasted for at least 4 h and were assessed in a supine position with their arm raised above the head for optimal intercostal exposure. 2D SWE was performed by using the Aixplorer US imaging system (SuperSonic Imagine, SSI, France). The examination was performed by experienced operators with >5 years of abdominal ultrasound and elastography scans. 2D-SWE was performed after a B-mode ultrasound scan, and the ROI (about 4 cm×3 cm) was set at 1–2 cm under the capsule of the right liver lobe (the 7th to 10th intercostal space) without large bile ducts and vessels [19] (Fig. 2). Five measurements were performed at the same location of the liver in each patient, and the mean of five LSMs was applied for analysis [19].

2.4. Liver histopathology

After partial hepatectomy, the nontumorous portion of liver tissue was evaluated by a consensus of two experienced pathologists without knowledge of the clinicoradiological data. Liver fibrosis and necroinflammatory activity were assessed according to the Scheuer scoring system [20], and steatosis was scored on a 4-point scale according to the fraction of hepatocytes with lipid droplets [14]. The hepatic fibrosis stages of ≥S2, ≥S3, and S4 were defined as significant fibrosis, advanced fibrosis, and cirrhosis, respectively.

2.5. Statistical analysis

Categorical variables were expressed as frequency and percentage. Quantitative variables were summarized as mean ± standard deviation

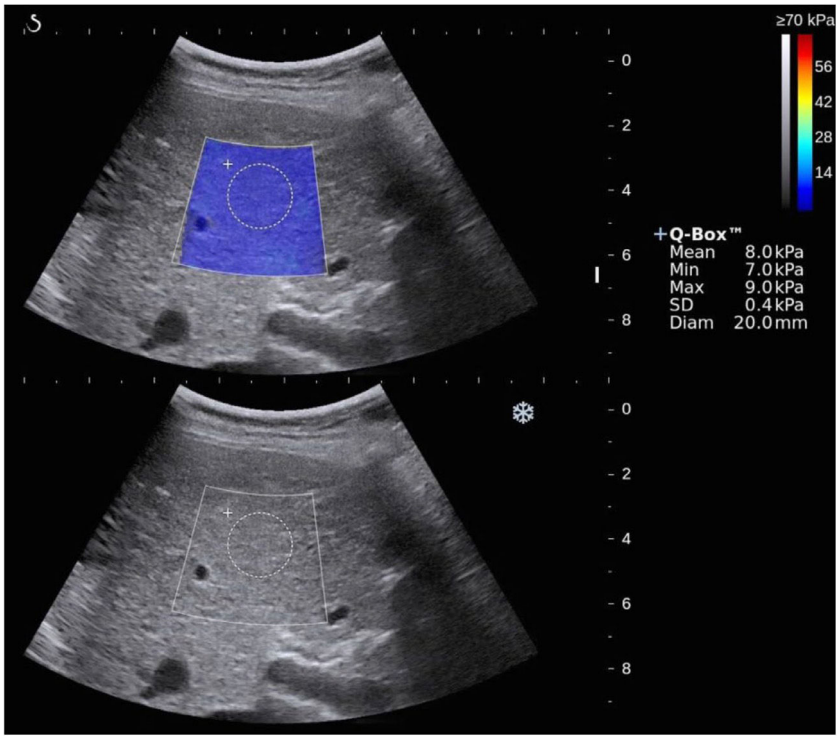

Fig. 2. The two-dimensional shear-wave elastography (top) and gray-scale (bottom) images of the right hepatic lobe in a patient.

or median and interquartile range (IQR) when appropriate. Interobserver agreement of measurements of μ_{Diff} was evaluated by using the intraclass correlation coefficient (ICC) with 95 % confidence interval (CI). The relationship between μ_{Diff} and LSM was measured by Spearman correlation analysis. The association between μ_{Diff} and LSM on one hand and histological fibrosis, necroinflammation, and steatosis on the other were explored by Spearman's rank correlation. The differences between μ_{Diff} and LSM among various extents of liver fibrosis were compared by using the Kruskal–Wallis test and post-hoc tests, and a Bonferroni-adjusted significance level of 0.005 (0.05/10) was applied. Receiver operating characteristic (ROC) curves were constructed to analyze the diagnostic capacity for significant fibrosis (≥S2), advanced fibrosis (≥S3), and cirrhosis (S4). Areas under the curves (AUCs) were compared with the Delong method [21]. All statistical analyses were performed using Medcalc 18.2.1 (Mariakerke, Belgium) and SPSS 23.0 (Chicago, IL, USA). $P < 0.05$ was considered statistically significant.

2.6. Ethical statements

Our Institutional Review Boards approved this retrospective study (Approval No B2021–430R). The study was conducted in accordance with the Ethical Principles for Medical Research Involving Human Subjects described in the 1975 Declaration of Helsinki as revised in 2000. The need for informed consent was waived.

3. Results

3.1. Patients' characteristics

The baseline characteristics of all patients enrolled are outlined in Table 1. Of all the patients, the leading etiology was hepatitis B/C (97/111, 87.4 %). The pathology of the focal liver lesions revealed malignant tumors in 99 patients (89.2 %) and benign lesions in 12 patients (10.8 %). According to Scheuer scoring system, the liver fibrosis was staged as S0 in 6 (5.40 %) patients, S1 in 8 (7.21 %) patients, S2 in 16 (14.41 %) patients, S3 in 19 (17.12 %) patients, S4 (55.86 %) in 62 patients; the inflammation activity grades were G0 in 4 (3.60 %), G1 in 29 (26.13 %), G2 in 66 (59.46 %) and G3 in 12 (10.81 %) patients. For steatosis, the numbers of the patients with scores 0, 1, 2 and 3 were 77 (69.37 %), 29 (26.13 %), 4 (3.60 %), and 1 (0.90 %), respectively.

3.2. DWI–based virtual shear modulus, 2D SWE, and histological findings

The interobserver agreements for μ_{Diff} between two radiologists were excellent (ICC=0.87, 95 % CI: 0.82–0.91). The median μ_{Diff} of each observer were 4.60 kPa (IQR: 4.20–5.20) and 4.70 kPa (IQR: 4.10–5.20), respectively. There was a significant positive correlation between μ_{Diff} and LSM (rho= 0.48, $P < 0.001$). μ_{Diff} (rho= 0.54, $P < 0.001$) and LSM (rho= 0.76, $P < 0.001$) were positively correlated with liver fibrosis stages, as well as necroinflammatory activity scores (rho= 0.24, $P = 0.01$; rho= 0.42, $P < 0.001$, respectively). However, μ_{Diff} ($r = 0.16$, $P = 0.10$) and LSM ($r = -0.08$, $P = 0.40$) were not associated with steatosis in hepatocytes.

The DWI–based virtual shear modulus and 2D SWE at each fibrosis stage are presented in Table 2 and Fig. 3. μ_{Diff} and LSM showed significant increases in S3 and S4 compared with S0, S1 and S2 ($P < 0.005$ for all), and LSM exhibited a significant difference between S3 and S4 ($P < 0.005$). Moreover, the LSM significantly increased in G2 and G3 compared to G0 and G1 ($P < 0.005$ for all). However, there were no significant differences in μ_{Diff} among various necroinflammatory activities ($P > 0.05$).

3.3. Diagnostic performance of DWI–based virtual shear modulus and 2D SWE

ROC curves of DWI–based virtual shear modulus μ_{Diff} and 2D SWE for liver fibrosis staging are shown in Fig. 4, with corresponding diagnostic test characteristics provided in Table 3. AUCs of μ_{Diff} for predicting significant fibrosis, advanced fibrosis, and cirrhosis were 0.81 (95 % CI: 0.73–0.88), 0.89 (95 % CI: 0.82–0.88), and 0.77 (95 % CI: 0.68–0.84), respectively. The AUCs of 2D SWE for diagnosing

Table 1
The baseline characteristics of all the patients.

	S0 (n = 6)	S1 (n = 8)	S2 (n = 16)	S3 (n = 19)	S4 (n = 62)
Age (years) ‡	51.5 ± 13.7	61.9 ± 9.7	56.3 ± 14.5	55.5 ± 10.2	55.0 ± 9.9
Male/Female	0/6	2/6	6/10	19/0	49/13
Body mass index (kg/m^2) ‡	23.2 ± 4.0	24.1 ± 4.3	22.6 ± 2.8	24.8 ± 3.2	24.5 ± 3.4
Liver disease etiology					
Hepatitis B/C	2 (33.3)	5 (62.5)	11 (68.8)	19 (100.0)	60 (96.8)
NAFLD	1 (16.7)	2 (25.0)	1 (6.2)	0	2 (3.2)
Other/unknown	3 (50.0)	1 (12.5)	4 (25.0)	0	
ALT*	11.5 (9.0–15.0)	18.0 (12.0–34.0)	20.0 (16.5–30.5)	34.0 (24.8–53.5)	28.0 (22.0–42.0)
AST*	17.5 (15.0–18.0)	21.0 (17.5–24.5)	24.5 (18.0–29.0)	26.0 (22.3–38.8)	28.5 (21.0–37.0)
Albumin‡	42.3 ± 4.3	43.0 ± 3.6	44.6 ± 3.7	42.3 ± 5.1	43.5 ± 4.9
Total bilirubin*	7.7 (6.9–11.3)	10.1 (6.1–13.4)	10.9 (8.2–12.8)	11.7 (9.3–13.7)	14.4 (10.4–18.5)
Necroinflammation					
G0	4 (66.7)	0	0	0	0
G1	2 (33.3)	7 (87.5)	5 (31.3)	5 (26.3)	10 (16.1)
G2	0	1 (12.5)	10 (62.5)	14 (73.70	41 (66.1)
G3	0	0	1 (6.2)	0	11 (17.8)
G4	0	0	0	0	0
Steatosis in hepatocytes					
<5 %	4 (66.7)	4 (50.0)	12 (75.0)	12 (63.2)	45 (72.6)
5 %–33 %	2 (33.3)	4 (50.0)	4 (25.0)	6 (31.6)	13 (21.0)
34 %–66 %	0	0	0	1 (5.2)	3 (4.8)
>67 %	0	0	0	0	1 (1.6)

NAFLD, non-alcoholic fatty liver disease; ALT, alanine aminotransferase; AST, aspartate aminotransferase.
Unless otherwise stated, data are the frequencies of patients, and numbers in parentheses are percentages.
‡ Data are the mean and standard deviation.
* Data are median and interquartile range in parentheses.

Table 2
DWI–based virtual shear modulus and two-dimensional SWE according to fibrosis stages and necroinflammatory activity.

Fibrosis	μ_{Diff} (kPa)	LSM (kPa)	Necroinflammation	μ_{Diff} (kPa)	LSM (kPa)
S0 (n = 6)	3.53 (2.70–4.05)	6.6 (6.1–6.9)	G0 (n = 4)	3.53 (3.10–3.80)	6.8 (6.4–7.0)
S1 (n = 8)	3.85 (3.08–4.53)	7.1 (6.1–7.7)	G1 (n = 29)	4.35 (3.75–5.08)	7.7 (6.6–10.8)
S2 (n = 16)	3.80 (3.40–4.18)	6.6 (5.8–7.5)	G2 (n = 66)	4.70 (4.10–5.20)	12.0 (9.0–15.0)
S3 (n = 19)	4.70 (4.51–5.28)	10.5 (9.1–12.6)	G3 (n = 12)	4.85 (4.38–5.73)	13.2 (11.8–14.7)
S4 (n = 62)	5.03 (4.35–5.40)	14.3 (10.8–16.1)	G4 (n = 0)	NA	NA
rho	0.54	0.76	rho	0.24	0.42
P	<0.001	<0.001	P	0.01	<0.001

μ_{Diff}, shear modulus obtained from DWI–based virtual elastography; LSM, liver stiffness measurement by two-dimensional shear wave elastography.
Data are median with interquartile range in parentheses.
There were significant differences of μ_{Diff} and LSM between S0 vs. S3, S0 vs. S4, S1 vs. S3, S1 vs. S4, S2 vs. S3, S2 vs. S4 ($P < 0.005$ for all), and there was a significant difference of LSM between S3 and S4 ($P < 0.005$).

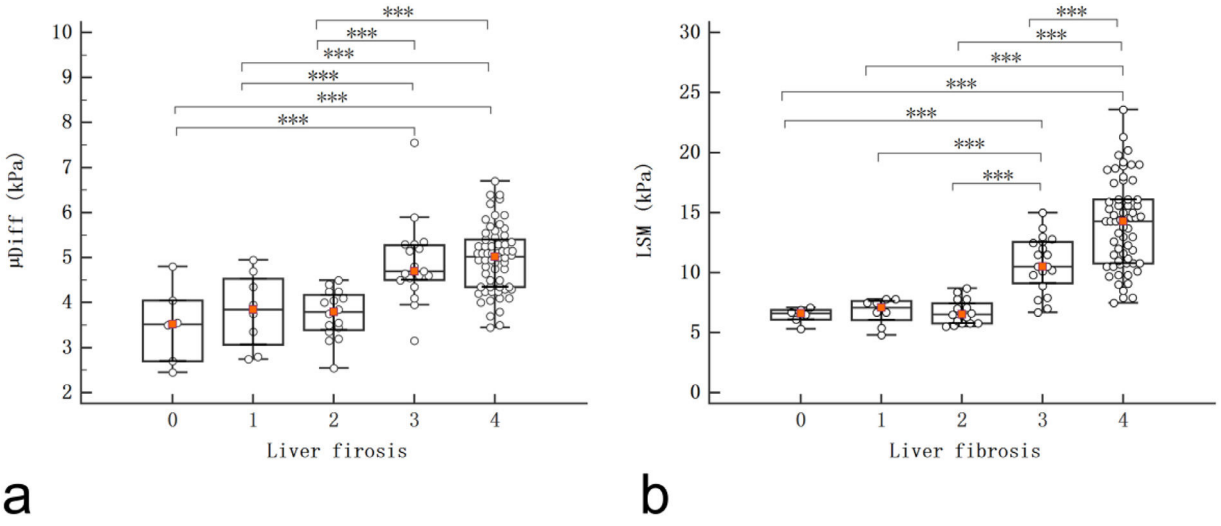

Fig. 3. The distributions of DWI-based virtual shear modulus (μ_{Diff}; a) and liver stiffness measurement (LSM) by two-dimensional shear-wave elastography (b) for various fibrosis stages. *** $P < 0.005$.

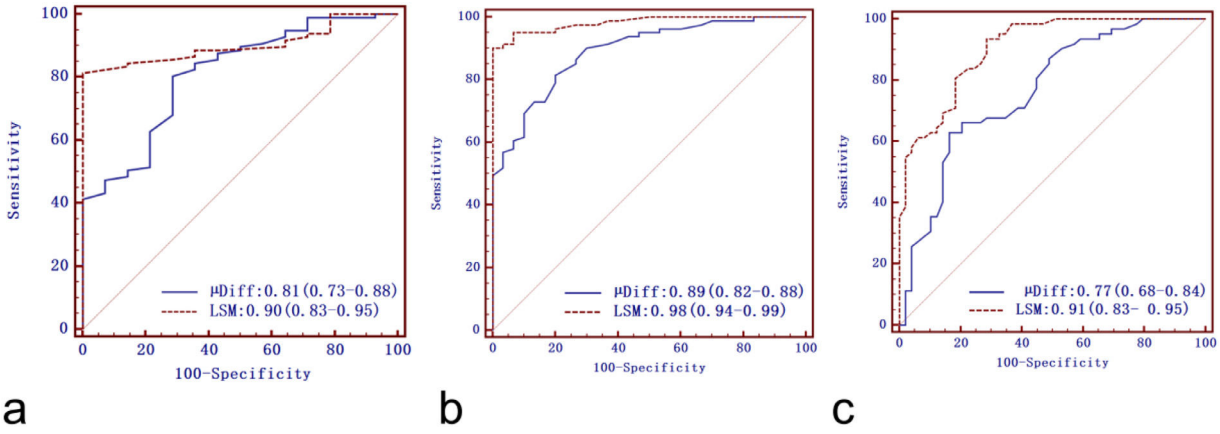

Fig. 4. Receiver operating characteristic curves of DWI-based virtual shear modulus (μ_{Diff}) and liver stiffness measurement (LSM) by two-dimensional shear-wave elastography for predicting significant fibrosis (a), advanced fibrosis (b) and cirrhosis (c). The aeras under the curves of the LSM were significantly higher than μ_{Diff} for advanced fibrosis and cirrhosis ($P < 0.05$ for both).

Table 3
Diagnostic test characteristics of DWI−based virtual elastography and two-dimensional shear wave elastography.

Modality and stage	AUC (95 %CI)	P value	Cutoff (kPa)	Sensitivity (%)	Specificity (%)
μ_{Diff}					
Stage 2 or greater	0.81 (0.73−0.88)	<0.001	>4.05	80.41 (71.1−87.8)	71.43 (41.9 - 91.6)
Stage 3 or greater	0.89 (0.82−0.94)	<0.001	>4.25	81.48 (71.3−89.2)	80.00 (61.4 - 92.3)
Stage 4	0.77 (0.68−0.84)	<0.001	>4.80	62.90 (49.7−74.8)	83.67 (70.3 - 92.7)
LSM					
Stage 2 or greater	0.90 (0.83−0.95)	<0.001	>7.8	81.44 (72.3 - 88.6)	100.00 (76.8 - 100.0)
Stage 3 or greater	0.98 (0.94−0.99)	<0.001	>8.7	90.12 (81.5 - 95.6)	100.00 (88.4 - 100.0)
Stage 4	0.91 (0.83- 0.95)	<0.001	>8.9	93.55 (84.3 - 98.2)	71.43 (56.7 - 83.4)

μ_{Diff}, shear modulus obtained from DWI−based virtual elastography; LSM, liver stiffness measurement by two-dimensional shear wave elastography.

significant fibrosis, advanced fibrosis, and cirrhosis were 0.90 (95 % CI: 0.83−0.95), 0.98 (95 % CI: 0.94−0.99) and 0.91 (95 % CI: 0.83-0.95), respectively. There were significantly higher AUCs in identifying advanced fibrosis and cirrhosis for LSM compared to μ_{Diff} ($P < 0.05$ for both). However, no significant difference in AUCs was observed between μ_{Diff} and LSM for detecting significant fibrosis ($P > 0.05$).

4. Discussion

We compared the diagnostic performance of DWI−based virtual shear modulus (μ_{Diff}) and LSM with 2D SWE for staging liver fibrosis in this study. Our results showed a significant positive correlation between μ_{Diff} and LSM. Furthermore, the AUCs of DWI−based virtual shear modulus were less than those of 2D SWE in identifying significant fibrosis, advanced fibrosis, and cirrhosis. Notably, LSM was superior to μ_{Diff} in predicting advanced fibrosis and cirrhosis.

DWI is capable of probing water movement, enabling noninvasive quantification of alterations in liver microstructure due to hepatic fibrosis [13,22]. Liver fibrosis is characterized by the accumulation of extracellular matrix, including collagen, which impedes the water motion in the liver. In the present study, we observed a significant positive correlation between histological liver fibrosis stages and μ_{Diff} estimated from DWI using b values of 200 and 1500 s/mm^2. The μ_{Diff} showed significant increases in S3 and S4 compared with S0, S1 and S2. The AUCs of μ_{Diff} for different stages of fibrosis were 0.77 −0.89 with sensitivity of 62.90 % to 81.48 % and specificity of 71.43 % to 83.67 %, which were comparable with Kromrey's results [18]. Previous studies have shown a significant association between water diffusivity and tissue elasticity in the liver [17,18], and Chen et al. [23] suggested that this relationship was probably linked to the tissue collagen content. The 2D SWE allows for noninvasive evaluation of hepatic fibrosis by measuring liver stiffness with high diagnostic accuracy (AUCs of 0.83−0.98) [11,19,24]. Our results also showed a strong correlation between LSM with 2D SWE and hepatic fibrosis, and LSM exhibited significant increases in S3 and S4 compared with S0, S1, and S2, as well as between S3 and S4. The AUCs of LSM for significant fibrosis, advanced fibrosis, and cirrhosis were 0.90,0.98 and 0.91, respectively, which were consistent with previous studies [11,19,24].

There was a significant positive correlation between μ_{Diff} and LSM. Kromrey et al. [18] reported a high agreement between μ_{MRE} and μ_{Diff} values and thus proposed DWI−based virtual MRE as an alternative to real MRE for fibrosis staging without the usage of compatible drivers. However, in Kromrey's studies, the gold standard for liver fibrosis was MRE rather than histology. In this study, histologic fibrosis stages were utilized as the reference standard. The comparison of AUCs demonstrated that 2D SWE was significantly superior to DWI−based virtual MRE in predicting advanced fibrosis and cirrhosis. 2D SWE has the particularity to display a real-time colored map of liver stiffness [24]. Quantified measurement of 2D SWE for hepatic stiffness directly relies on the content and microstructure of fiber components that alter with the progression of liver fibrosis [25]. In contrast, DWI−based virtual MRE is associated with water diffusivity, and the latter is determined by the amount of extracellular matrix that changes through the severity of fibrosis [17,18]. DWI sequence may be affected by artifacts such as blurring and susceptibility, thereby leading to inferior results. Although larger AUCs were observed in LSM than in μ_{Diff} for assessing significant fibrosis, the diagnostic performance was not significantly different. This may be attributed to the limited number of patients included in S0 and S1.

Our study had some limitations. Firstly, this is a retrospective study, which may introduce patient selection bias. Secondly, we used resected liver specimens instead of liver biopsies for histological

assessments. The liver tissue in the resected sample was significantly larger than in the liver biopsy, and the histologic fibrosis staging may be more objective [19]. Thirdly, the number of patients in each fibrosis stage group was not uniform. Half of the patients had cirrhosis, as liver neoplasms typically occur in patients with cirrhosis [19]. Lastly, the DWI sequence is sensitive to blurring, motion, and susceptibility artifacts, which may compromise the estimation of $\mu_{\text{Diff.}}$ However, we have excluded the patients with evident image artifacts. Further prospective external studies are warranted to validate the DWI-based virtual elastography for liver fibrosis staging.

5. Conclusions

Our study highlights that LSM by 2D SWE yields larger AUCs than μ_{Diff} obtained from DWI-based virtual elastography for various stages of liver fibrosis. LSM is superior to μ_{Diff} in predicting advanced fibrosis and cirrhosis.

Data availability statement

The authors confirm that the data supporting the findings of this study are available within the article.

Funding

This work was supported by the Youth Project of National Natural Science Foundation of China (Grant No. 82202112), Youth Project of Natural Science Foundation of Fujian Province (Grant No. 2023J05293), Youth Foundation of Shanghai Municipal Health Commission (Grant No. 20204Y0346), National Natural Science Foundation of China (Grant No. 82171897, 82371923), Natural Science Foundation of Shanghai (Grant No. 21ZR1459700). The funding agencies had no role in the design and conduct of the study, collection, analysis, and interpretation of the data, nor did they prepare the manuscript.

Author contributions

Li Yang was responsible for Writing-original draft; Guofeng Zhou handled Data curation; Liheng Liu and Shengxiang Rao were responsible for Methodology; Wentao Wang and Kaipu Jin handled Formal analysis; Caixia Fu managed Software; Mengsu Zeng and Ying Ding contributed to Conceptualization. The scientific guarantor of this publication is Ying Ding.

Declaration of interests

None.

Acknowledgments

We'd like to thank Yuan Zhuang for providing help on 2D SWE.

Supplementary materials

Supplementary material associated with this article can be found in the online version at doi:10.1016/j.aohep.2024.101743.

References

[1] Devarbhavi H, Asrani SK, Arab JP, Nartey YA, Pose E, Kamath PS. Global burden of liver disease: 2023 update. J Hepatol 2023;79:516–37. https://doi.org/10.1016/j.jhep.2023.03.017.

[2] European Association for the Study of the Liver. Electronic address eee. Clinical practice guideline P, chair, representative EGB, Panel m. EASL clinical practice guidelines on non-invasive tests for evaluation of liver disease severity and prognosis - 2021 update. J Hepatol 2021;75:659–89. https://doi.org/10.1016/j.jhep.2021.05.025.

[3] Sun Y, Chen W, Chen S, Wu X, Zhang X, Zhang L, et al. Regression of liver fibrosis in patients on hepatitis B therapy is associated with decreased liver-related events. Clin Gastroenterol Hepatol 2024;22:591–601. https://doi.org/10.1016/j.cgh.2023.11.017.

[4] Parola M, Pinzani M. Liver fibrosis in NAFLD/NASH: from pathophysiology towards diagnostic and therapeutic strategies. Mol. Aspects Med. 2023;95:101231. https://doi.org/10.1016/j.mam.2023.101231.

[5] Shipley LC, Axley PD, Singal AK. Liver fibrosis: a clinical update. Hepatology (Baltimore, Md) 2019;7:105–17. https://doi.org/10.1002/hep.22742.

[6] Rockey DC, Caldwell SH, Goodman ZD, Nelson RC, Smith AD. American association for the study of liver D. Liver biopsy. Hepatology (Baltimore, Md) 2009;49:1017–44. https://doi.org/10.1002/hep.22742.

[7] Ichikawa S, Goshima S. Gadoxetic acid-enhanced liver MRI: everything you need to know. Invest Radiol 2024;59:53–68. https://doi.org/10.1097/RLI.0000000000000990.

[8] Guglielmo FF, Barr RG, Yokoo T, Ferraioli G, Lee JT, Dillman JR, et al. Liver fibrosis, fat, and iron evaluation with mri and fibrosis and fat evaluation with US: a practical guide for radiologists. Radiographics 2023;43:e220181. https://doi.org/10.1148/rg.220181.

[9] Abeysekera KWM, Valenti L, Younossi Z, Dillon JF, Allen AM, Nourredin M, et al. Implementation of a liver health check in people with type 2 diabetes. Lancet Gastroenterol Hepatol 2024;9:83–91. https://doi.org/10.1016/S2468-1253(23)00270-4.

[10] Jang JK, Lee ES, Seo JW, Kim YR, Kim SY, Cho YY, et al. Two-dimensional shear-wave elastography and us attenuation imaging for nonalcoholic steatohepatitis diagnosis: a cross-sectional, multicenter study. Radiology 2022;305:118–26. https://doi.org/10.1148/radiol.220220.

[11] Kakegawa T, Sugimoto K, Kuroda H, Suzuki Y, Imajo K, Toyoda H, et al. Diagnostic accuracy of two-dimensional shear wave elastography for liver fibrosis: a multicenter prospective study. Clin Gastroenterol Hepatol 2022;20:e1478–82. https://doi.org/10.1016/j.cgh.2021.08.021.

[12] Li J, Lu X, Zhu Z, Kalutkiewicz KJ, Mounajjed T, Therneau TM, et al. Head-to-head comparison of magnetic resonance elastography-based liver stiffness, fat fraction, and T1 relaxation time in identifying at-risk NASH. Hepatology (Baltimore, Md) 2023;78:1200–8. https://doi.org/10.1097/HEP.0000000000000417.

[13] Taouli B, Koh DM. Diffusion-weighted MR imaging of the liver. Radiology 2010;254:47–66. https://doi.org/10.1148/radiol.09090021.

[14] Leitao HS, Doblas S, Garteiser P, d'Assignies G, Paradis V, Mouri F, et al. Hepatic fibrosis, inflammation, and steatosis: influence on the MR viscoelastic and diffusion parameters in patients with chronic liver disease. Radiology 2017;283:98–107. https://doi.org/10.1148/radiol.2016151570.

[15] Huang J, Leporq B, Hervieu V, Dumortier J, Beuf O, Ratiney H. Diffusion-weighted MRI of the liver in patients with chronic liver disease: a comparative study between different fitting approaches and diffusion models. J Magn Reson Imaging 2024;59:894–906. https://doi.org/10.1002/jmri.28826.

[16] Jang W, Jo S, Song JS, Hwang HP, Kim SH. Comparison of diffusion-weighted imaging and MR elastography in staging liver fibrosis: a meta-analysis. Abdom Radiol (NY) 2021;46:3889–907. https://doi.org/10.1007/s00261-021-03055-2.

[17] Le Bihan D, Ichikawa S, Motosugi U. Diffusion and intravoxel incoherent motion mr imaging-based virtual elastography: a hypothesis-generating study in the liver. Radiology 2017;285:609–19. https://doi.org/10.1148/radiol.2017170025.

[18] Kromrey ML, Le Bihan D, Ichikawa S, Motosugi U. Diffusion-weighted MRI-based Virtual Elastography for the Assessment of Liver Fibrosis. Radiology 2020;295:127–35. https://doi.org/10.1148/radiol.2020191498.

[19] Zhuang Y, Ding H, Zhang Y, Sun H, Xu C, Wang W. Two-dimensional shear-wave elastography performance in the noninvasive evaluation of liver fibrosis in patients with Chronic Hepatitis B: comparison with serum fibrosis indexes. Radiology 2017;283:873–82. https://doi.org/10.1148/radiol.2016160131.

[20] Scheuer PJ. Classification of chronic viral hepatitis: a need for reassessment. J Hepatol 1991;13:372–4. https://doi.org/10.1016/0168-8278(91)90084-o.

[21] DeLong ER, DeLong DM, Clarke-Pearson DL. Comparing the areas under two or more correlated receiver operating characteristic curves: a nonparametric approach. Biometrics 1988;44:837–45 PMID:3203132.

[22] Park JH, Seo N, Chung YE, Kim SU, Park YN, Choi JY, et al. Noninvasive evaluation of liver fibrosis: comparison of the stretched exponential diffusion-weighted model to other diffusion-weighted MRI models and transient elastography. Eur Radiol 2021;31:4813–23. https://doi.org/10.1007/s00330-020-07600-3.

[23] Chen Y, Li R, Yang Y, Ma D, Zhou J, Wang C, et al. Correlation analysis of structural and biomechanical properties of hepatocellular carcinoma tissue. J Biomech 2022;141:111227. https://doi.org/10.1016/j.jbiomech.2022.111227.

[24] Paisant A, Lemoine S, Cassinotto C, de Ledinghen V, Ronot M, Irles-Depe M, et al. Reliability criteria of two-dimensional shear wave elastography: analysis of 4277 measurements in 788 patients. Clin Gastroenterol Hepatol 2022;20:400–8 e10. https://doi.org/10.1016/j.cgh.2020.12.013.

[25] Lu Q, Lu C, Li J, Ling W, Qi X, He D, et al. Stiffness value and serum biomarkers in liver fibrosis staging: study in large surgical specimens in patients with Chronic Hepatitis B. Radiology 2016;280:290–9. https://doi.org/10.1148/radiol.2016151229.